

Thermoelectric efficiency in the space-charge-limited transport regime in semiconductors

François Léonard*
(Dated: August 9, 2018)

The thermoelectric efficiency of semiconductors is usually considered in the ohmic electronic transport regime, which is achieved through high doping. Here we consider the opposite regime of low doping where the current-voltage characteristics are nonlinear and dominated by space-charge-limited transport. We show that in this regime, the thermoelectric efficiency can be described by a single figure of merit, in analogy with the ohmic case. Efficiencies for bulk, thin film, and nanowire materials are discussed, and it is proposed that nanowires are the most promising to take advantage of space-charge-limited transport for thermoelectrics.

I. INTRODUCTION

Most implementations of thermoelectric devices utilize highly doped semiconductors with linear (ohmic) current-voltage characteristics. In such materials, the thermoelectric efficiency is determined by the figure of merit $zT = S^2\sigma T/\kappa$ where S is the Seebeck coefficient, σ the electrical conductivity, T the temperature, and κ the thermal conductivity. The zT factor has governed much of the research in developing approaches to improve thermoelectric efficiency; however, the intimate relationship between transport quantities places constraints on the possible paths towards efficiency improvements. Thus, new approaches where the thermoelectric efficiency does not depend on zT would open new routes for scientific exploration.

An example of such an approach is thermionic cooling and power generation, which was originally considered for injection into vacuum[1], and then into semiconductors[2]. These thermionic devices are often considered different from thermoelectric devices due to the presence of an injection barrier and because the channel length is shorter than the electronic mean-free path, giving ballistic electron transport[3-5]. However, as the channel length increases beyond the mean-free path, thermionic devices become equivalent to thermoelectric devices[6, 7], which has led to new proposals to engineer multilayer semiconductor materials[8].

In this manuscript, we explore an alternative approach that does not rely on ohmic transport or thermionic emission, but instead exploits space-charge-limited (SCL) electronic transport in a semiconductor. We derive an expression for thermoelectric efficiency in this regime, and show that it depends on a new dimensionless figure of merit that replaces zT . Furthermore, we apply the theory to bulk, thin film, and nanowire materials, and conclude that nanowires are the most promising to harness SCL transport for thermoelectrics.

The term "space-charge-limited" originated from the

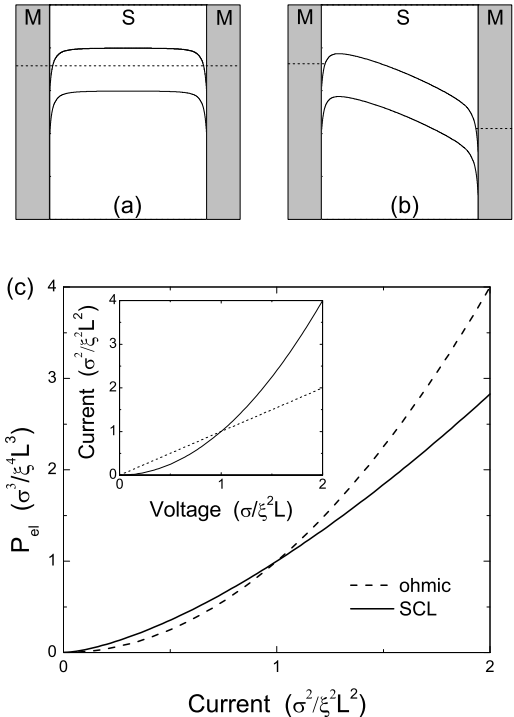


FIG. 1: Panels (a) and (b) show band diagrams for a metal-semiconductor-metal system when the semiconductor has low doping. Figure (a) is at equilibrium while figure (b) is under an applied voltage. Solid lines are the valence and conduction band edges and dashed lines are the Fermi levels. (c) Power loss due to Joule heating plotted for ohmic transport and for SCL transport in dimensionless units. The inset shows the current-voltage characteristics for these two transport regimes.

consideration of charge injection into a region where electronic transport is ballistic. In that case, space-charge effects are detrimental because they create an additional barrier for injection compared with the reference space-charge-free system[9]. This situation is relevant to *thermionic* devices where space-charge effects have been shown to reduce efficiency[1]. The issue of space-charge is different if one considers semiconductor-based *thermoelectric* devices. There, the reference system is a highly-doped semiconductor with two ohmic contacts. In that

*Electronic address: fleonar@sandia.gov

case, space-charge effects are minimal because the high doping immediately screens the injected charge. However, if the doping in the semiconductor is lowered, space charge effects become dominant, and the current becomes larger than the ohmic current because electronic transport is no longer determined by the free-carrier relaxation time, but by the shorter carrier transit time[9]. This situation, which has been observed experimentally in a broad range of materials, is the one that we consider in this manuscript.

Figure 1 shows the system under consideration: a low-doped semiconductor between two ohmic contacts. Band diagrams are shown in Figs 1a,b for the case relevant to electron injection: the metal Fermi level contacts the semiconductor in the conduction band creating a large density of carriers in the near-interface region. Band-bending away from the metal/semiconductor interface creates a barrier for electron injection at zero bias. Under bias, a maximum in the potential is created near the injecting electrode, defining the so-called "virtual cathode"[10]. Modeling has demonstrated that in the presence of this virtual cathode, SCL transport dominates as soon as the applied bias V exceeds a few kT [11]. This leads to a current-voltage relationship $J \propto V^2$ as discussed further below. This relationship differs from the exponential $J - V$ characteristics usually considered for thermionic systems[1]; the transitions between the thermionic and SCL regimes and the role of Schottky barriers has been studied in detail[12, 13], demonstrating that SCL dominates even when small Schottky barriers are present.

II. THERMOELECTRIC EFFICIENCY

To be specific, we consider the thermoelectric power generation efficiency of the system of Fig. 1, but the approach should apply to cooling as well. The efficiency of a thermoelectric material for power generation is given by[14]

$$\eta = \frac{P_{th} - P_{el}}{Q} = \frac{J \int_{T_c}^{T_h} S(x) dT - J \int_0^L \nabla v(x) dx}{JT_h S_h + \kappa_h \nabla T_h} \quad (1)$$

where P_{th} is the thermoelectric power generated, P_{el} is the electrical power dissipated, and Q is the thermal power supplied. Here T_c and T_h are the cold and hot side temperatures and $v(x)$ is the local potential.

Usually, one considers a highly doped semiconductor of length L between ohmic contacts. For a bias voltage V , there is a linear drop of the potential along the channel due to the free-carrier screening; this leads to $J = \sigma V/L$, giving $P_{el} = J^2 L/\sigma$ and the dependence of the efficiency on zT [14]. For SCL transport, the transport equations need to be solved self-consistently with the Poisson equation due to the unscreened space-charge[15]; in the simplest model with diffusive electronic transport[15], this gives an electrostatic potential that depends on position

as

$$v(x) = (x/L)^{3/2} V. \quad (2)$$

This nonlinear spatial dependence of the potential leads to the current-voltage relationship [15]

$$J = \xi^2 V^2. \quad (3)$$

Thus, in the SCL regime, the current is no longer linear in V , but is quadratic instead. The proportionality constant ξ depends on the dimensionality of the material, and to some extent on the shape of the electrodes, as will be discussed further below.

The quadratic form of the $J - V$ behavior implies that $P_{el} = J^3/\xi$; the interest in this transport regime for thermoelectrics is illustrated in Fig. 1c, where P_{el} for the ohmic and SCL regimes are compared. There, P_{el} in the SCL regime is below that of the ohmic regime at sufficiently high voltage, suggesting a potentially new regime of operation for thermoelectrics. (The cross-over between ohmic and SCL transport occurs at $V_c = \sigma/\xi^2 L$, as shown in the Fig. 1c inset. This sets a condition for when ohmic contributions should be negligible compared to SCL transport.)

To derive the thermoelectric efficiency in this regime, we utilize the approach described in Ref. [14]. From the above equations we obtain for the local efficiency

$$d\eta(x) = \frac{dT}{T} \frac{S - \frac{3}{2} \frac{J^{1/2}}{\xi \Delta T} \left(\frac{x}{L}\right)^{1/2}}{S + \kappa \nabla T / T J} = \frac{dT}{T} \eta_r(x, T), \quad (4)$$

where we used $dP_{el} = J dv(x)$, and where the prefactor dT/T indicates that the efficiency is limited by the Carnot efficiency. The temperature T depends on position through the heat equation[16]

$$\frac{d(\kappa \nabla T)}{dx} = -T \frac{dS}{dT} J \nabla T - \frac{3}{2} \frac{J^{3/2}}{\xi L} \left(\frac{x}{L}\right)^{1/2}. \quad (5)$$

The first term on the right hand side is the usual Thomson effect, while the second term is the local Joule heating in the material dP_{el} . This equation applies for SCL transport because both the electronic and phononic transport are diffusive, and thus both the electronic and phononic thermal conductivities are well defined (this has been demonstrated for SCL transport in nanowires[17]).

The total efficiency of a segment is obtained from[18]

$$\eta = 1 - \exp \left[- \int_{T_c}^{T_h} \frac{\eta_r(x, T)}{T} dT \right]. \quad (6)$$

Noticing that $d \ln (ST + \kappa \nabla T / J) / dT = [S + d(\kappa \nabla T / J) / dT] / [ST + \kappa \nabla T / J]$ and assuming that the coefficients are independent of temperature and position we arrive at

$$\eta = 1 - \frac{S_c T_c + \kappa \nabla T_c / J}{S_h T_h + \kappa \nabla T_h / J}. \quad (7)$$

Thus, the efficiency depends only on quantities evaluated at the cold and hot sides[14]. To obtain these quantities we integrate the heat equation to get

$$\begin{aligned} \kappa \nabla T_c / J &= \frac{\kappa}{J} \left(\frac{\Delta T}{L} + \frac{2}{5} \frac{J^{3/2}}{\xi \kappa} \right) \\ \kappa \nabla T_h / J &= \frac{\kappa}{J} \left(\frac{\Delta T}{L} - \frac{3}{5} \frac{J^{3/2}}{\xi \kappa} \right) \end{aligned} \quad (8)$$

which leads to

$$\eta = \frac{\Delta T}{T_h} \frac{y^2 (1-y)}{y^2 + \frac{1}{g\bar{T}} \frac{T_h}{\Delta T} - \frac{3}{5} \frac{\Delta T}{T_h} y^3} \quad (9)$$

where

$$y = \left(\frac{J}{S^2 \xi^2 (\Delta T)^2} \right)^{1/2} \quad (10)$$

and

$$g\bar{T} = \frac{S^3 \xi^2 L T_h^2}{\kappa}. \quad (11)$$

The variable y is a dimensionless quantity equal to the ratio between the generated voltage and the maximum thermoelectric voltage that can be developed across the material. $g\bar{T}$ is a dimensionless parameter that replaces the zT factor from conventional ohmic materials. (Note that the average temperature \bar{T} does not directly appear in $g\bar{T}$. However, we use the notation \bar{T} as a reminder that, as a first approximation, the quantities that enter $g\bar{T}$ should be evaluated at the average temperature across the material.)

Figure 2 shows the dependence of the efficiency on y from Eq. (9), indicating that positive efficiency is achieved in the range $0 < y < 1$, with a maximum attained at an intermediate value. This behavior is similar to that obtained for conventional ohmic losses[14], but with a different functional dependence.

The maximum efficiency is obtained by maximizing η with respect to y to obtain

$$\frac{g\bar{T}}{2} \frac{\Delta T}{T_h} \left(1 - \frac{3}{5} \frac{\Delta T}{T_h} \right) y^3 + \frac{3}{2} y - 1 = 0. \quad (12)$$

This equation provides the optimal $y(g\bar{T}, \Delta T/T_h)$ that maximizes the efficiency:

$$y^* = \frac{1}{2\epsilon} \delta - \frac{1}{\delta} \quad (13)$$

where $\delta = \sqrt{\epsilon} [4\sqrt{\epsilon} + 2\sqrt{2}\sqrt{1+2\epsilon}]^{1/3}$ and $\epsilon = \frac{g\bar{T}}{2} \frac{\Delta T}{T_h} \left(1 - \frac{3}{5} \frac{\Delta T}{T_h} \right)$. At this optimal y the efficiency is

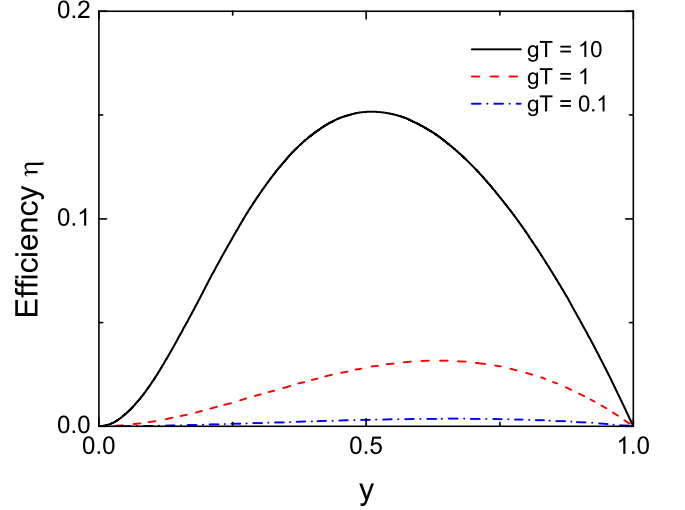


FIG. 2: Thermoelectric efficiency as a function of variable y for three values of the $g\bar{T}$ factor.

given by

$$\eta = \frac{\Delta T}{T_h} \frac{1 - \frac{3}{2} y^*}{1 - \frac{9}{10} \frac{\Delta T}{T_h} y^*}. \quad (14)$$

Thus, the efficiency only depends on $g\bar{T}$ and $\Delta T/T_h$, much like ohmic materials where the dependence is on zT and $\Delta T/T_h$.

Figure 3a shows the calculated efficiency as a function of $g\bar{T}$ for $\Delta T/T_h = 1/2$, indicating low efficiency at small $g\bar{T}$ and efficiencies approaching the Carnot efficiency at large $g\bar{T}$. The two limiting cases of small and large $g\bar{T}$ can be obtained as

$$\eta = \begin{cases} \frac{\Delta T}{T_h} \left[1 - 3 \left(\frac{1}{2} - \frac{3}{10} \frac{\Delta T}{T_h} \right)^{2/3} \left(\frac{\Delta T}{T_h} g\bar{T} \right)^{-1/3} \right] & \text{large } \frac{\Delta T}{T_h} g\bar{T} \\ \frac{4}{27} \left(\frac{\Delta T}{T_h} \right)^2 g\bar{T} & \text{small } \frac{\Delta T}{T_h} g\bar{T} \end{cases} \quad (15)$$

thus providing simple analytical expressions for these two regimes. The small $(\Delta T/T_h) g\bar{T}$ expression provides a good estimate of the full curve up to about 1% efficiency, while the large $(\Delta T/T_h) g\bar{T}$ approximation is valid for $\eta \gtrsim 20\%$.

The inset in Fig. 3a shows the efficiency for a traditional ohmic material as a function of zT for $\Delta T/T_h = 1/2$, where $zT = 1$ gives about 10% efficiency. Since this is the current state-of-the-art in thermoelectric materials, we can use it as a comparison with the SCL regime; in that case one would need $g\bar{T} \approx 5$ to achieve the same efficiency at this given $\Delta T/T_h$. However, the efficiency depends significantly on $\Delta T/T_h$, as shown in Fig. 3b for values of $g\bar{T}$ as high as 10. The curve for $g\bar{T} = 1$ is well approximated by the small $(\Delta T/T_h) g\bar{T}$ limit of Eq. (15), indicating a quadratic dependence on $\Delta T/T_h$.

The full expression for $g\bar{T}$ depends on the parameter ξ , which in turn depends on the dimensionality of the

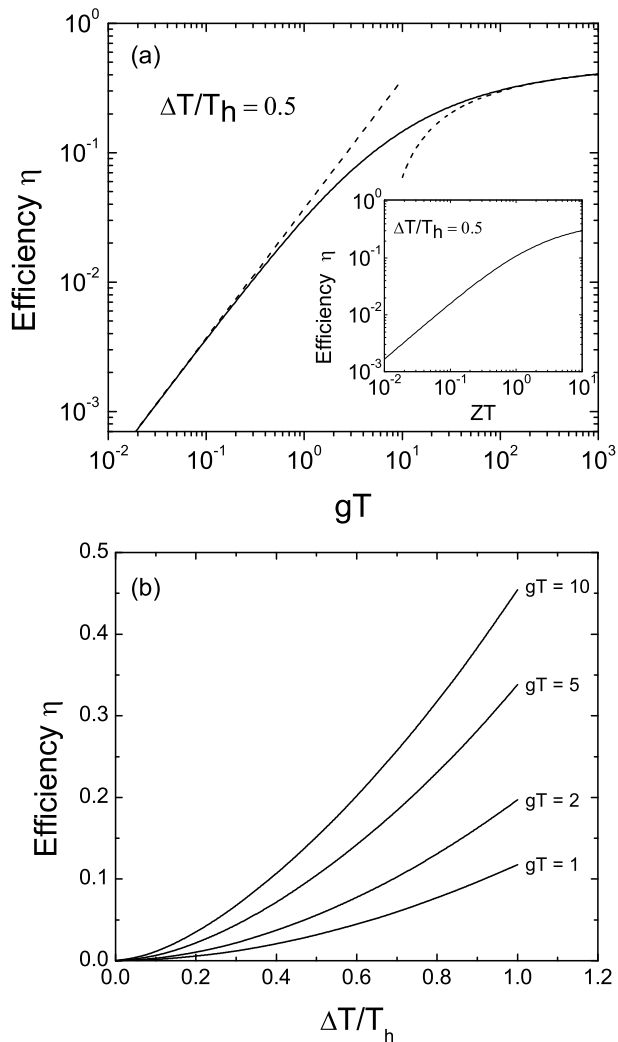


FIG. 3: (a) Thermoelectric efficiency as a function of the $g\bar{T}$ factor. Dashed lines are the low and high $g\bar{T}$ behaviors from Eq. (15). Inset is the efficiency as a function of zT . (b) Thermoelectric efficiency as a function of $\Delta T/T_h$.

material under consideration; for bulk[15], thin film[15], and nanowire[19] materials, it is given by

$$\xi^2 = \begin{cases} \frac{9\varepsilon\mu}{8L^3} & \text{bulk} \\ \xi_0 \frac{\varepsilon\mu}{tL^2} & \text{thin film, } t \ll L \\ \xi \frac{\varepsilon\mu}{R^2L} & \text{nanowire, } R \ll L \end{cases} \quad (16)$$

where ε is the permittivity, μ is the mobility, and ξ_0 is a numerical constant that depends on the shape of the electrodes, equal to 1 for planar contacts[15]. t is the thickness of the thin film, while R is the nanowire radius (see Fig. 4 for illustrations of the different geometries.) The expressions for the thin film and nanowire cases are applicable when $t/L \ll 1$ and $R/L \ll 1$; for larger values of t/L and R/L , ξ crosses over to the bulk expression[19].

The $g\bar{T}$ factor also depends on the material parameters S , κ , μ , and ε . Like traditional ohmic materials, high $g\bar{T}$ requires large S , low κ and large μ ; but it also

needs large ε , a criterion not usually required for high zT . This arises because large ε serves to screen the injected charge, and reduces the repulsive Coulomb interaction that opposes charge injection. This is beneficial because dielectric screening maintains the SCL transport regime, in contrast to free-carrier screening that would make the current ohmic.

Two advantages of the SCL regime are that the maximum values of S and μ can be exploited. Indeed, ohmic materials are usually operated at high doping where both S and μ are reduced from their maximum values. But at low doping S attains a maximum at a value[20] $S \approx E_g/2e\bar{T}$ while μ saturates to its intrinsic value μ_{int} . We can thus write the maximum value of $g\bar{T}$ as

$$g\bar{T} = \left(\frac{E_g}{2e\bar{T}} \right)^3 \frac{a\varepsilon\mu_{int}L\bar{T}_h^2}{\kappa} \quad (17)$$

where a is a geometry-dependent factor that can be obtained from Eq. (16). We note that the $g\bar{T}$ factor depends linearly on μ , just like an ohmic material where $zT \sim \sigma \sim \mu$; however, the difference is that the mobility in zT is the high-doping mobility, which is smaller than μ_{int} .

III. PRACTICAL ESTIMATES

To evaluate the practicality of the SCL approach for thermoelectric power generation, we apply the theory to the bulk, thin film, and nanowire geometries for $T_h = 600$ K and $\Delta T = 300$ K. We consider GaAs at low doping as an example material since SCL has been observed in this material[21], and because material properties are readily available[22]: at $\bar{T} = 450$ K and low doping, $E_g = 1.35$ eV, $\varepsilon = 13$, $\mu \approx 3150$ cm²/V S , and $\kappa \approx 30$ W/mK. Figure 4a shows the calculated efficiency for a bulk device as a function of the channel length L . The efficiency is low unless L is very small. The case of thin films (Fig. 4b) is slightly more promising with larger efficiencies at longer lengths, but this requires small film thicknesses. Also note that the large ΔT over the small lengths L where reasonable efficiency is observed in Fig. 4a and 4b would lead to very large heat fluxes that further limit the usefulness of these geometries. Thus, for the bulk or thin film geometries to be useful, a much larger $g\bar{T}$ is needed so they can operate at longer lengths, and this would require other or new materials with better properties for SCL thermoelectrics.

The situation is significantly more favorable if one considers nanowires, as shown in Fig. 4c. In that case, SCL currents are enhanced due to the scaling $\xi^2 \sim R^{-2}L^{-1}$; in fact, $g\bar{T}$ becomes independent of length, and scales as R^{-2} , with R being naturally small for nanowires. This leads to a large efficiency which exceeds the 10% value for nanowires less than 20nm in radius. This efficiency could be even larger if other effects predicted and measured for nanowires were included; for example, from Eq. (17), $g\bar{T}$

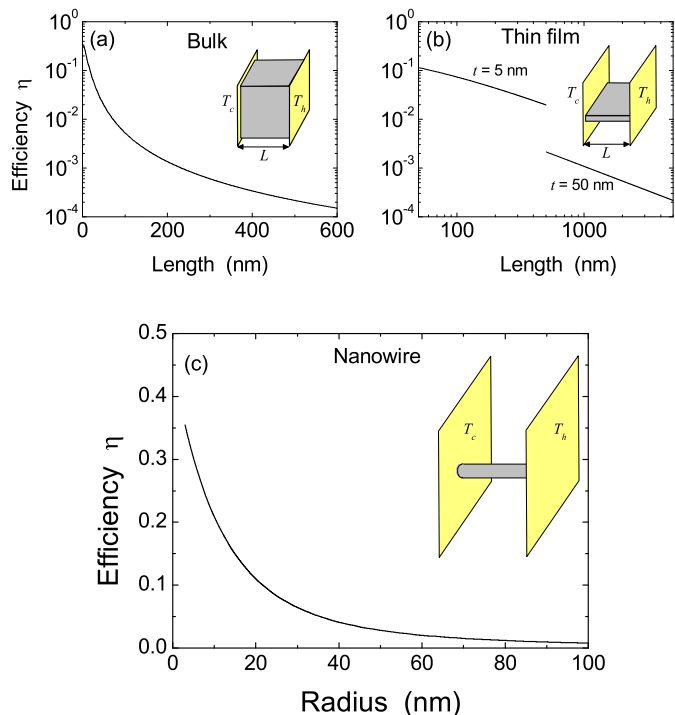


FIG. 4: Thermoelectric efficiency at $T_h = 600K$ and $\Delta T = 300K$ for (a) bulk material as a function of length, (b) thin film material as a function of length for two thicknesses, and (c) nanowire as a function of radius. In (b), the curves are plotted for $t < L/10$ to satisfy the criterion $t \ll L$ (see Eq. 16).

depends sensitively on the bandgap, which increases with decreasing diameter. Similarly, the thermal conductiv-

ity is reduced with decreasing nanowire diameter, which could also make $g\bar{T}$ larger. It should be noted that the electrical currents needed to achieve the efficiency plotted in Fig. 4c are less than a μA per nanowire and require voltages on the order of a volt, which is easily achieved without damaging the nanowires or the contacts[19].

IV. CONCLUSION

In summary, we considered the efficiency of thermoelectric materials in the space-charge-limited regime and found that it depends on a single dimensionless parameter $g\bar{T}$, in analogy with conventional ohmic materials. When applied to bulk, thin film and nanowire geometries, we find that nanowires are the most promising to harness SCL transport. This work provides a new path for improving the performance of thermoelectric materials, and suggests the exploration of new thermoelectric materials with properties conducive to SCL transport.

V. ACKNOWLEDGEMENT

Discussions with Peter Sharma and Doug Medlin are gratefully acknowledged. This project is supported by the Laboratory Directed Research and Development program at Sandia National Laboratories, a multiprogram laboratory managed and operated by Sandia Corporation, a wholly owned subsidiary of Lockheed Martin Corporation, for the United States Department of Energy's National Nuclear Security Administration under Contract DE-AC04-94AL85000.

*email: fleonar@sandia.gov

-
- [1] G. Mahan, J. Appl. Phys. **76**, 4362 (1994).
 - [2] A. Shakouri, Annu. Rev. Mater. Res. **41**, 399 (2011).
 - [3] G. S. Nolas, J. Sharp, and H. J. Goldsmid, *Thermoelectrics Basic Principles and New Materials Developments* (Springer, Berlin, 2001).
 - [4] M. D. Ulrich, P. A. Barnes, and C. B. Vining, J. Appl. Phys. **90**, 1625 (2001).
 - [5] G. D. Mahan, J. O. Sofo, and M. Bartkowiak, J. Appl. Phys. **83**, 4683 (1998).
 - [6] G. D. Mahan, J. Appl. Phys. **87**, 7326 (2000).
 - [7] T. Zeng and G. Xhen, J. Appl. Phys. **92**, 3152 (2002).
 - [8] M. F. O'Dwyer, T. E. Humphrey, R. A. Lewis, and C. Zhang, J. Phys. D: Appl. Phys. **39**, 4153 (2006).
 - [9] M. A. Lampert and P. Mark, *Charge Injection in Solids* (Academic Press, New York, 1970).
 - [10] A. Rose, Phys. Rev. **97**, 1538 (1955).
 - [11] A. A. Grinberg and S. Luryi, J. Appl. Phys. **61**, 1181 (1987).
 - [12] P. S. Davids, I. H. Campbell, and D. L. Smith, J. Appl. Phys. **82**, 6319 (1997).
 - [13] W. Chandra, L. K. Ang, and W. S. Koh, J. Phys. D: Appl. Phys. **42**, 055504 (2009).
 - [14] G. J. Snyder and T. S. Ursell, Phys. Rev. Lett. **91**, 148301 (2003).
 - [15] A. A. Grinberg, S. Luryi, M. R. Pinto, and N. L. Schryer, IEEE Trans. Electron Devices **36**, 1162 (1989).
 - [16] The heat equation for nanowires is discussed in F. Léonard, Appl. Phys. Lett. **98**, 103101 (2011).
 - [17] A. M. Katzenmeyer *et al*, IEEE Trans. Nanotech. **10**, 92 (2011).
 - [18] T. C. Harman and J. M. Honig, *Thermoelectric and Thermomagnetic Effects and Applications* (McGraw-Hill, New York, 1967).
 - [19] A. A. Talin, F. Léonard, B. S. Swartzentruber, X. Wang, and S. D. Hersee, Phys. Rev. Lett. **101**, 076802 (2008).
 - [20] H. J. Goldsmid and J. W. Sharp, J. Electron. Mater. **28**, 869 (1999).
 - [21] J. W. Allen and R. J. Cherry, Nature **189**, 297 (1961).
 - [22] J. S. Blakemore, J. Appl. Phys. **53**, R123 (1982).